

# S-N and Crack Initiation Fatigue Models for Computation of Landing Gear Life

Krishna L S<sup>\*</sup>, Rakshith M<sup>+</sup>, and Prashant S H<sup>+</sup>

<sup>\*</sup>CSIR-National Aerospace Laboratories, Structural Technologies Division, Bengaluru.

<sup>+</sup>CMR Institute of Technology, Department of Mechanical Engineering, Bengaluru.

\*kls@nal.res.in

---

## ABSTRACT

*Fatigue failure occurs due to the application of fluctuating/ service stresses that are about one order less than the stress required to cause failure under ramp application of load. The Stress-Life (S-N) and Crack Initiation Fatigue Models include Goodman, Gerber, Morrow, None and Smith-Watson-Topper (SWT). In this paper, an elementary beam and landing gear analyzed for static and fatigue. The various stress combination and a methodology for fatigue analysis presented in this paper.*

**Keywords:** FE analysis, Fatigue analysis, Stress-life, Crack initiation, Landing gear.

---

## 1. INTRODUCTION

Fatigue life computation has become an important part of the aerospace structure, especially in the landing gear design. However, multiaxial fatigue remains a domain approached by a limited number of specialists in the numerical or experimental computation of life. In the field of High Cycle Fatigue (HCF) many components from industries with strategic importance (such as aerospace and nuclear) are operating in the HCF domain and early or unexpected failures can have catastrophic or accidents leading to claiming lives or injuries. It is essential to know which model needs to be used for the computation of fatigue life.

## 2. DEVELOPMENT OF FE MODELS

In this paper, two problems were discussed. First an elementary cantilever beam and second the landing gear problem. For the first elementary cantilever beam the model is created from scratch, but for the LG imported the CAD model. After importing cleaning the geometry for the extra curves are removed.

### 2.1 Material properties

There are two material properties (Table 1) [3] used in this paper. First steel used for both the elementary problem and for the landing gear. In the landing gear, only the toggle links are made of aluminium material.

### 2.2 Loading and BC

The cantilever beam is loaded at the tip (45 N) and fixed at the other end. The landing gear is fixed at the pintle pin and actuator end. The loading is provided on the axle (vertical and drag), side loads applied using MPC as tire model. For more details on loading and boundary conditions refer 0.

**Table 1.1 Mechanical and Fatigue properties**

<b>Mechanical Properties</b>	<b>Aluminium-2014-T6 SAE 1529 Steel</b>	
Ultimate Tensile strength (MPa)	483	1005
Yield Strength (MPa)	437	902
Young’s Modulus (GPa)	72.7	207
Poisson’s ratio	0.334	0.3
<b>Fatigue Properties:</b>		
$S_{f'}$ : Fatigue Strength coefficient(MPa)	976	1253
b : Fatigue strength exponent	-0.12	-0.08
c : Fatigue ductility exponent	-0.88	-0.36
$E_{f'}$ : Fatigue ductility coefficient	0.88	0.07
n’: Cyclic strain hardening exponent	0.049	0.2
K’: Cyclic strength coefficient(MPa)	605	2118

**3. LINEAR STATIC ANALYSIS**

Elements used in the analyses are 1D (Beam), 2D (Shell), and 3D (Hexa, Tetra hydra). All the elements are of the continuous compatibility type. Nastran Solution number 101 for static analysis used.

**4. FE BASED FATIGUE ANALYSIS**

Most of the problems are multiaxial in nature. It is essential to have equivalent stress approach 0. The von Mises equivalent stress as a function of time, given by the Eq. 1

$$\sigma_{eq}(t) = \frac{1}{\sqrt{2}} \sqrt{\{\sigma_x(t) - \sigma_y(t)\}^2 + \{\sigma_y(t) - \sigma_z(t)\}^2 + \{\sigma_z(t) - \sigma_x(t)\}^2 + 6(\tau_{xy}^2 + \tau_{yz}^2 + \tau_{xz}^2)} \quad (1)$$

$\sigma_{eq}(t)$  von Mises does not retain the negative stress values. To eliminate this limitation Bishop 0 proposed a correction. The equivalent stress of von Mises became “signed von Mises” stress 0, the sign being generally given by the first principal stress, its general form is given in Eq. 2

$$\sigma_{eq\ vMs}(t) = \sigma_{eq}(t) \cdot sign(I_1(t)) \quad (2)$$

Where  $I_1 = \sigma_x + \sigma_y + \sigma_z$

It is stated and plotted by Dumitru et al 0, that the  $\sigma_{eq}(t)$  does not correctly reflect there all load spectrums and cannot be considered as a substitute for the given stress components, since it does not retain the negative stress values.

For 10000 cycles, Stress ratio R = -1. The cantilever beam problem rendered a life of 6.29 whereas the conventional von Mises equivalent stress is 1E20. Enter the offset value in the load magnitude row; thereby the load applied increase or decrease.

#### 4.1 Load Normalizing, and Offsets

The Finite Element stress results from a sub case is scaled in three different ways **Error! Reference source not found.** using the (i) Load Magnitude (B), (ii) Scale Factor (A) and (iii) Offset (C). Here in this used only the load magnitude and offset. The stress time or cyclic variation is determined as in Eq. 3

$$\sigma_{ij}(t) = P(t) \frac{A\sigma_{ij}}{B} + C \quad (3)$$

Where, P (t) = cyclic load as a variation of time;  $\sigma_{ij}$  = stress tensor from the sub case; A = scale factor; B = load magnitude; C = offset

#### 4.2S-N Fatigue Models

From the perspective of applied cyclic stresses, the fatigue damage of a component strongly correlates with the applied stress amplitude or applied stress range, and is secondarily influenced by the mean stress. In the case of a fully reversed loading case the mean stress effect is zero. Various theories used for the consideration of mean stress effects are briefly discussed in this document. Goodman relation Eq. 4[8]is commonly used due to the mathematical simplicity and slightly conservative results. The Gerber relation is quadratic as gave in Eq. 5[8]. $\sigma_a$  – alternating stress,  $\sigma_m$  – mean stress,  $\sigma_f$  – fully reversed (R = -1) fatigue strength,  $\sigma_u$  – ultimate stress, and None Eq. 6 [8](No mean stress correction).

$$\text{Goodman: } \frac{\sigma_a}{\sigma_f} + \frac{\sigma_m}{\sigma_u} = 1 \quad (4)$$

$$\text{Gerber: } \frac{\sigma_a}{\sigma_f} + \left( \frac{\sigma_m}{\sigma_u} \right)^2 = 1 \quad (5)$$

$$\text{None: } \frac{\Delta\sigma}{2} = \sigma_a = \sigma'_f (2N_f)^b \quad (6)$$

$\sigma'_f$  – Fatigue strength coefficient, b – fatigue strength exponent.

#### 4.3Crack Initiation Models

Crack Initiation: Life to initiate a crack (i) Morrow Eq. 7, (ii) S-W-T Eq. 8, and (iii) None (No mean stress applied) Eq. 9

$$\text{Morrow: } \frac{\Delta\varepsilon}{2} = \varepsilon_a = \frac{\sigma'_f - \sigma_m}{E} (2N_f)^b + \varepsilon'_f (2N_f)^c \quad (7)$$

$\sigma_m$  is the mean stress.

$$\text{S-W-T: } \sigma_{\max} \varepsilon_a E = (\sigma'_f)^2 (2N_f)^{2b} + \sigma'_f \varepsilon'_f E (2N_f)^{b+c} \quad (8)$$

$$\text{None: } \frac{\Delta\varepsilon}{2} = \varepsilon_a = \frac{\sigma'_f}{E} (2N_f)^b + \varepsilon'_f (2N_f)^c \quad (9)$$

### 5. MATLAB SCRIPTS FOR FATIGUE ANALYSIS

MATLAB script (\*.m) code files were written using the expression of Goodman, Gerber, Morrow, Smith-Watson and Topper (SWT)0, and None. These scripts are applicable at a single point of maximum stress.

## 6. RESULTS AND DISCUSSION

Figure 1 and 2 render stress and displacement fringe patterns. Table 2 depicts the percentage error in these stress and displacement values.

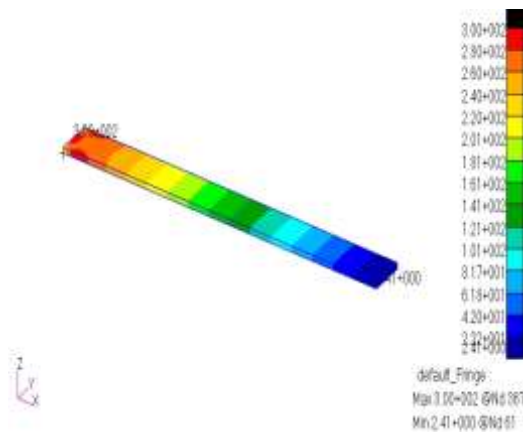


Figure 1.1 Stress values from static analysis

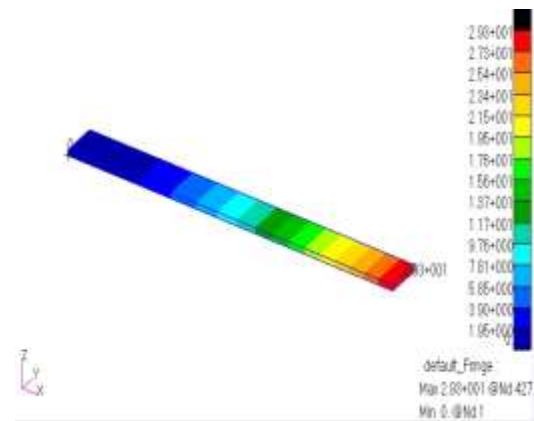


Figure 1.2 Displacement magnitudes

Table 1.2 Cantilever beam static analysis results

Description	Patran	Theoretical	Error
<b>von Mises Stress(MPa)</b>	300	300	0.0%
<b>Displacement (mm)</b>	29.3	29.55	0.87%

Table 1.3 show the stress/ strain combination option available for both S-N and Crack initiation analyses. In this paper the table 3 results represent for the S-N Goodman analysis. They are fourteen options available; in this paper only eight have been discussed. The following eight stress/ strain options are (i) Maximum Absolute Principal, (ii) Maximum Principal, (iii) Minimum Principal, (iv) Signed von Mises, (v) von Mises, (vi) Signed maximum Shear, (vii) Signed Tresca, and (viii) Critical Plane. The minimum principal and von Mises stress combination show infinite life (1E20 or 1E8, Fig. 3). These should not be considered. Usually in the linear static analysis von Mises stress is generally considered and it has been accepted. In the Fatigue life analysis only von Mises render very poor result. The next two stress combinations are signed maximum shear and signed Tresca these two render same results (1E20), again these two need not to be considered. Maximum Principal Stress renders 1E20. The signed von Mises is better (3.20E7, Fig. 4). For the fatigue analysis it is recommended to use Maximum absolute principal or critical plane stress combinations only for good results in this case these both render 7.14E6. However, the stress combination depends on the loading conditions. Table 4 indicates the S-N, crack initiation and MATLAB results for maximum absolute principal stress combination. Figures 5 and 6 represents 1D and 3D stress contour models of main landing gear (MLG) for inclined reaction, loading cases, respectively.

Table 1.3 Fatigue life of cantilever beam for various stress combinations

S. N.	Stress Combination	MSC Fatigue (1cycle)	MATLAB (1cycle)	MSC Fatigue (10000 cycles)
1	Max. Abs. Principal	7.14E6	2.63E7	7.14E2
2	Max. Principal	1E20	2.5E12	1E20
3	Min. Principal	1E20	4.84E13	1E20
4	Signed von Mises	3.20E7	8.3E7	3.20E3
5	von Mises	1E20	1E20	1E20
6	Signed Max Shear	1E20	7.54E12	1E20
7	Signed Tresca	1E20	7.54E12	1E20
8	Critical Plane	7.14E6	2.63E7	7.14E2

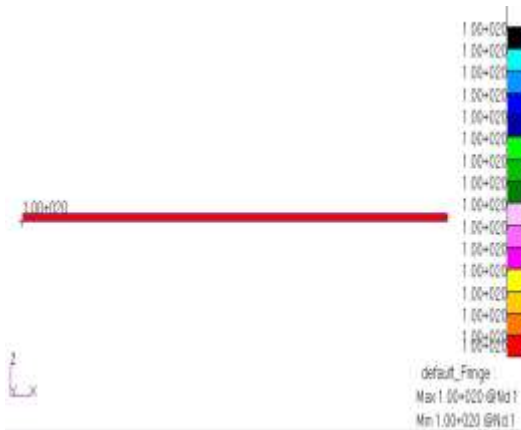


Figure 1.3 Fatigue life using von Mises stress combination

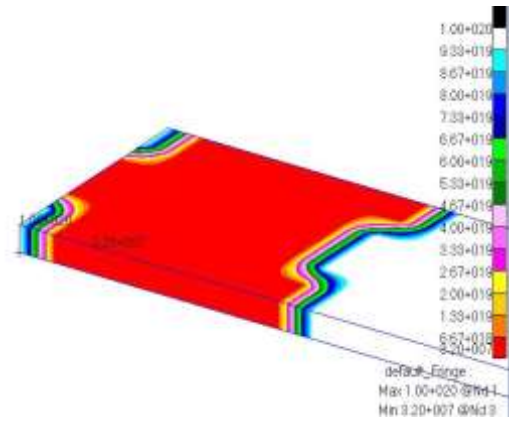


Figure 1.4 Fatigue life using Signed von Mises stress combination

Table 1.4 Patran and MATLAB results comparison for S-N and Crack initiation analysis

Fatigue model	MSC Patran	MATLAB	Model	Patran	MATLAB
Goodman	7.14E6	2.61E7	SWT	3.39E7	4.91E7
Gerber	8.33E6	2.61E7	Morrow	4.28E7	6.41E7
None	8.34E6	9.39E6	None	4.56E7	6.41E7

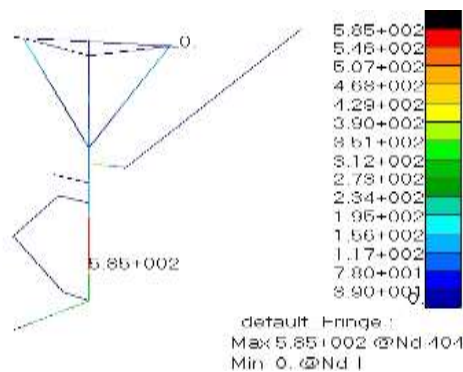


Figure 1.5 MLG 1D von Mises stress contours

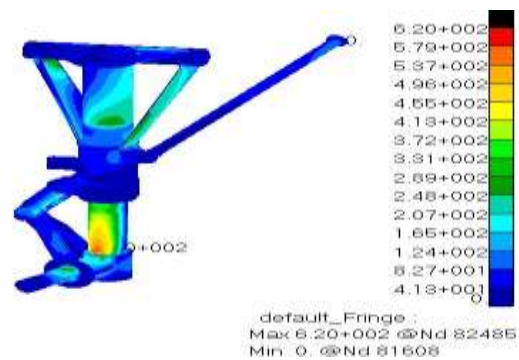


Figure 1.6 MLG 3D von Mises stress contours

## 7. CONCLUSION

Developed FE models for elementary and landing gear, carried out Static and Fatigue analyses. Excellent comparison of results obtained for static analyses. In the case of fatigue analysis the number of applied cycles in loading history increases, fatigue life in cycles decreases proportional to loading history cycles. Among the various stress combination maximum absolute principal stress, critical plane, and signed von Mises render better results. In the fatigue sensitivity analysis by providing offset value equal to yield value of the material the morrow fatigue life indicated value is less than 10% deviation, further work is in progress.

## REFERENCES

- [1] Andres I Gustavsson, Measurement of Landing gear loads of a commuter airline, 1986, ICAS-86-5.9.3, Sweden.
- [2] Feng, J., Titus, P., Proposed Method for Evaluating Multiaxial Fatigue in ITER, PSFC/RR-07-4, Plasma Science and Fusion Center MIT, Cambridge, U.S.A., 2007.
- [3] MSC Nastran 2014, Nastran Embedded Fatigue User's Guide, www.mscsoftware.com, November 13, 2014.
- [4] Krishna Lok S and Abdul Waheed A (2015), Stress and Fatigue Damage Computation of a Nose Landing Gear, International Journal of Fracture and Damage Mechanics (IJFDM) Vol. 1: Issue 1, 16-33, 23July2015.
- [5] Bishop, J.E., Characterizing the non-proportional and out-of-phase extent of tensor paths, Fatigue Fract. Eng.Mater. Struct., 23 (2000) 1019-1032.

- [6] Kun Lorand, Review of high cycle fatigue models applied for multi axial tension-torsion loading based on new accuracy assessment parameter, Journal of Engineering Studies and Research – Vol. 18, No.3, 2012, pp. 75-86.
- [7] Dumitru Ion, Kun Lorand, DreuceanMircea, MenyhardtKarloly, The Equivalent Stress concept in Multiaxial Fatigue, Journal of Engineering Studies and Research – Volume 17 (2011) No. 2 53.
- [8] S.Suresh, Fatigue of materials, second edition, Cambridge University press, UK, 1998. ISBN 0 521 57847 7 (pbk.).
- [9] Shariati M, Mehrabi H, Energy-Based Predictions of Low-Cycle Fatigue Life of CK45 Steel and SS316 Stainless Steel, Journal of Solid Mechanics, Vol. 6, No. 3 (2014) pp. 278-288.